Revolutions in lipid isomer resolution: application of ultra-high resolution ion mobility to reveal lipid diversity

Berwyck L.J. Poad*,[1,2,3] Lachlan J. Jekimovs,[2] Reuben S.E. Young,[2†] Puttandon Wongsomboon,[2] David L. Marshall,[1,3] Felicia Hansen,[2] Therese Fulloon,[2,3] Michael C. Pfrunder,[2,3] Tyren Dodgen,[4] Mark Ritchie,[5] Stephen C.C. Wong,[5] Stephen J. Blanksby*[1,2,3]

[1]Central Analytical Research Facility, Queensland University of Technology, Australia, [2]School of Chemistry and Physics, Queensland University of Technology, Australia, [3]Centre for Materials Science, Queensland University of Technology, Australia, [4]Waters Australia, [5]Waters Pacific Pte. Ltd., Singapore.

*Corresponding authors

ABSTRACT: Many families of lipid isomers remain unresolved by contemporary liquid chromatography-mass spectrometry approaches, leading to a significant underestimation of structural diversity within the lipidome. While ion-mobility coupled to mass spectrometry has provided an additional dimension of lipid isomer resolution, some isomers require resolving power beyond the capabilities of conventional platforms. Here we present the application of high-resolution travelling-wave ion mobility for the separation of lipid isomers that differ in (i) the location of a single carbon-carbon double bond, (ii) the stereochemistry of the double bond (*cis* or *trans*) or, for glycerolipids, (iii) the relative substitution of acyl chains on the glycerol backbone (*sn*-position). Collisional activation following mobility separation allowed identification of carbon-carbon double bond position and *sn*-position, enabling confident interpretation of variations in mobility-peak abundance. To demonstrate the applicability of this method, double bond and *sn*-position isomers of an abundant phosphatidylcholine composition were resolved in extracts from a prostate cancer cell line and identified by comparison to pure isomer reference standards, revealing the presence of six isomers. These findings suggest that ultra-high resolution ion-mobility has broad potential for isomer-resolved lipidomics and is attractive to consider for future integration with other modes of ion-activation, thereby bringing together advanced orthogonal separations and structure elucidation to provide a more complete picture of the lipidome.

INTRODUCTION

Lipids are ubiquitous molecular components of all living systems where they perform a staggering array of diverse cellular functions ranging from the assembly of membranes to energy storage, transport and signaling. Understanding the lipidome requires a detailed knowledge of the structure-function relationships of each lipid within a cell or organism. This presents the analytical challenge of elucidating the molecular structure of individual lipids within a complex background of hundreds, or even thousands, of similar but non-identical compounds.[1, 2] Significant advances in chromatography-mass spectrometry over the last 20 years have underpinned major advances in our knowledge of the diversity of lipids present in nature, their biosynthetic origins and their interactions with other lipids and proteins.[3, 4] Despite these gains, one of the challenges peculiar to lipidomics has been the separation and unique identification of lipid isomers that share the same elemental formula and differ only in their molecular structures.[5] This analytical challenge results from the –often subtle– structural variation between isomers. In glycerophospholipids for example, structural variants can arise from (i) different combinations of fatty acyl chains; (ii) the connectivity of the acyl chains to the glycerol backbone (*sn*-position); (iii) variable sites(s) of unsaturation and; (iv) geometry about carbon-carbon double bonds (*i.e.*, *cis* or *trans* stereochemistry). The inability of most contemporary lipidomics workflows to resolve isomers differing in one (or a combination) of these dimensions leads to an underestimation of the overall diversity of the lipidome and knowledge gaps such as the metabolic origins and biological function(s) of the lipids themselves.

Chromatographic approaches, including gas- and liquid-chromatography, can provide resolution of some isomeric lipids, however the timescale of these separations is on the order of minutes or even can be up to hours to separate some structural isomers.[6] While structurally powerful, such separations present a bottleneck for high-throughput analyses. In recent years, ion mobility (IM) coupled to mass spectrometry (MS) has provided a rapid way to separate lipid isomers on a timescale compatible with fast chromatography, [7-10] as well as experimental workflows where prior separation is not possible (*e.g.*, in MS-imaging).[11] Conventional ion mobility platforms, however, lack the necessary resolving power to separate isomeric species with only subtle variations in molecular structure. As a result, recent instrument developments that have improved IM-resolution are gaining attention in a number of applications,[12-15] including for separating isomeric lipids.[10, 16, 17]

Once separated by mobility or chromatography, the challenge of unique identification of lipids remains. Often, tandem mass spectrometry employing low energy collision-

induced dissociation (CID) is used, since this is available on many commercial instruments and can be used to provide information about the building blocks of complex lipids, including information on lipid class and acyl chain composition. In many cases however, CID of mass-selected lipid ions does not provide structurally diagnostic product ions to unequivocally identify the lipid. Offline derivatization strategies have been developed for liquid chromatography mass spectrometry (LC-MS) workflows to enhance sensitivity and promote the formation of structurally diagnostic CID product ions.[18, 19] Recently it has been shown that some of these derivatization methods can be also be deployed to enhance ion mobility separation identification of isomeric lipids.[20, 21]

Here we deploy ultra-high resolution cyclic ion mobility spectrometry coupled with mass spectrometry to separate and identify isomers across several classes of lipid, namely fatty acyls (FAs), lysophosphatidylcholine (LPC) and diacyl phosphatidylcholine (PC). The strategy is then applied to profile the isomeric composition of two prostate cancer cell lines, revealing the presence of up to six isomeric lipids sharing the PC 34:1 composition.

EXPERIMENTAL METHODS

Lipid Nomenclature: Nomenclature and shorthand notations used here principally follows the recommendations of the LipidMAPS consortium.[22] Where a fatty acid has been derivatized to a 3-pyridylcarbinol ester, the shorthand annotation for the fatty acid is prepended with 3PE (*e.g.*, 3PE-FA18:1). Carbon-carbon double bond position(s) in acyl chains are indicated using the '*n-x*' nomenclature, where *x* indicates the double bond position relative to the methyl end of the acyl chain.[23] Where known, the stereochemistry of the carbon-carbon double bond is indicated as *cis* or *trans*.

Samples and preparation: Fatty acid standards FA18:1*n*-9(*cis*) and FA18:1*n*-9(*trans*) were purchased from Tokyo Chemical Industry (Tokyo, Japan), while FA18:1*n*-7(*cis*) and FA18:1*n*-7(*trans*) were purchased from Merck (Truganina, VIC). These four isomeric fatty acids were derivatized to 3-pyridylcarbinol ester derivatives following a previously described procedure.[24, 25] Briefly, dry tetrahydrofuran (50 μL) was added to potassium *tert*-butoxide (5.6 mg, yielding a ca. 1 M solution) followed by 3-pyridyl methanol (100 μL). After the reagent mixture turned clear the fatty acid (~5 mg in 1 mL dry dichloromethane) was added and heated at 45 °C for 45 min. After cooling to ambient temperature, water (1 mL) and hexane (2 mL) was added to the solution and then vortexed. The organic (top) layer was collected and washed with water (1 mL) and the organic (top) layer collected again. Residual water was removed using anhydrous sodium sulphate and filtered. The resulting solvent was removed by evaporating under nitrogen. Samples were then reconstituted to 0.5 μM in methanol for mass spectrometry analysis.

Isomers of lysophosphatidylcholine 1-oleoyl-2-hydroxy-*sn*-glycero-3-phosphocholine (LPC 18:1*n*-9(*cis*)/0:0) and 1-hydroxy-2-oleoyl-*sn*-glycero-3-phosphocholine (LPC 0:0/18:1*n*-9(*cis*)) were purchased from Avanti Polar Lipids (Alabaster, AL) and diluted to a concentration of 1.0 μM in methanol. Isomerically pure phosphatidylcholine standards 1-palmitoyl-2-(11Z-octadecenoyl)-glycero-3-phosphocholine (IsoPure PC 16:0/18:1*n*-7(*cis*)), 1-(11Z-octadecenoyl)-2-palmitoyl-*sn*-glycero-3-phosphocholine (IsoPure PC 18:1*n*-7(*cis*)/16:0), 1-palmitoyl-2-oleoyl-glycero-3-phosphocholine (IsoPure PC 16:0/18:1*n*-9(*cis*)), 1-oleoyl-2-palmitoyl-*sn*-glycero-3-phosphocholine (IsoPure PC 18:1*n*-9(*cis*)/16:0), 1-palmitoyl-2-(8Z-octadecenoyl)-*sn*-glycero-3-phosphocholine (IsoPure PC 16:0/18:1*n*-10(*cis*)), 1-(8Z-octadecenoyl)-2-palmitoyl-*sn*-glycero-3-phosphocholine (IsoPure PC 18:1*n*-10(*cis*)/16:0), were obtained from Avanti Polar Lipids and diluted to a concentration of 0.5 μM in methanol.

Lipids were extracted from LNCaP cells (Accession CVCL_0395) following a previously published protocol.[26] The extracted lipids were reconstituted in methanol for mass spectrometry analysis.

Mass Spectrometry: Experiments were conducted on a Cyclic Ion Mobility (cIMS) enabled quadrupole time-of-flight mass spectrometer (Waters Select Series; Wilmslow, UK). Details of the cIMS and its operation have been described previously,[12, 27] and only a brief description of the methods used is detailed here. Samples were injected using an autosampler (Waters Acquity Premier *UPLC*; 10 μL injection volume) into 20 μL min^{-1} flow of methanol. No chromatography column was used. Precursor ions were mass selected by the quadrupole before passing to the ion storage array. Packets of the mass selected ions were injected into the cIMS device and separated over multiple passes. Details of the cyclic sequence parameters used are provided in the supporting information (Table S1). Following IMS separation, the ions were collisionally activated in the transfer region prior to mass analysis by time of flight. Acquired data was processed using a combination of DriftScope (version 3.0) and MassLynx (version 4.2) with extracted ion arrival time distributions (ATDs) created using the measured *m/z* with a tolerance of ±0.05.

RESULTS

A methanolic mixture of FA18:1*n*-7(*cis*), FA18:1*n*-7(*trans*), FA18:1*n*-9(*cis*) and FA18:1*n*-9(*trans*)) infused using electrospray ionization in negative ion mode yielded abundant signal for the deprotonated fatty acid at *m/z* 281. Mass selection of the $[M-H]^-$ precursor ion and subsequent ion mobility separation provided broad separation of the *cis*/*trans* double bond geometry isomers after 10 passes around the cIMS device, however only minimal separation was observed between double bond positional isomers (Figure S1). Based on individual injections, the peak-to-peak resolving power[28] for the *cis*/*trans* isomer pairs is R_{pp}~0.75, while between the *cis* or *trans* pairs (*e.g.* FA18:1*n*-7(*cis*) *vs* FA18:1*n*-9(*cis*)) was R_{pp}~0.22 and 0.34, respectively. Moreover, the low energy CID spectra of deprotonated fatty acids are uninformative with respect to double bond position or geometry.

In typical gas chromatography workflows, fatty acids are derivatized to reduce their respective boiling points and aid chromatographic separation. Similar strategies have also been deployed in liquid chromatography to enhance sensitivity and promote the formation of structurally diagnostic product ions in MS/MS workflows.[18, 19] One such derivative

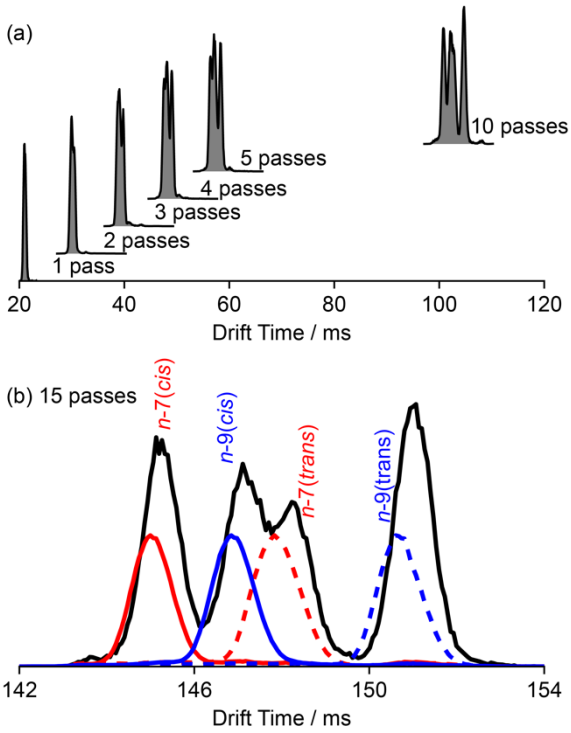

Figure 1. (a) Arrival time distributions for an infusion of a 4-component mix of fatty acids derivatized as 3-pyridylcarbinol esters after multiple numbers of passes around the cyclic IMS device, (b) IMS trace after 15 passes, overlaid with normalized arrival time distributions for individual injections of each isomer.

is a pyridylcarbinol ester, where a pyridine moiety is esterified to the carboxylic acid end of the fatty acid.[29] Following this logic, the same set of four FA isomers were derivatized as 3-pyridylcarbinol esters and infused as a methanol solution via electrospray ionization in positive ion mode. Precursor ions (*m/z* 374) were mass selected by the quadrupole and subsequently separated over multiple passes around the cIMS device. The resulting arrival time distributions after 1 – 10 passes around the cyclic ion mobility device are presented in Figure 1(a). After a single pass around the IMS device, only a single arrival time distribution was observed. Increasing the number of passes led to the formation of a shoulder, which separated into 4 distinct arrival time features after 15 passes. Comparison of the mixture to individual injections of the derivatized fatty acid isomers (Figure 1(b)) indicated that the ordering of the ATD peaks was 3PE-FA18:1*n*-7(*cis*), 3PE-FA18:1*n*-9(*cis*), 3PE-FA18:1*n*-7(*trans*) and 3PE-FA18:1*n*-9(*trans*). Notably, the ordering of arrival times is the same as that observed when the same four derivatized fatty acids are separated by reversed-phase liquid chromatography, and consistent with experimentally determined relative CCS values from drift tube IMS. Although the relative CCS of the 2 *cis* isomers differ by <0.4% (and the 2 *trans* isomers differ by <0.7%),[30] these 3-PE derivatives are distinctly separated after 15 passes on the cIMS device. While the same relative arrival time ordering was observed for the respective deprotonated free fatty acids (Figure S1), derivatization increased R_{pp} to ~1.0 for the two *cis* isomers. Recent spectroscopic measurements of the 3-PE derivatives, supplemented by density functional theory calculations, have identified that a charge-olefin interaction between the FA double bond and the protonated pyridyl group significantly impacts the gas-phase structure.[30] In the absence of this interaction, the isomeric free fatty acid anions are not separated as efficiently.

Confident in the capacity of the cIMS to separate structurally similar lipid isomers, we next examined a different form of isomerism encountered in glycerophospholipids, namely regioisomers differing in the (*sn*-)position of acyl chains on the glycerol backbone. We first considered lysophosphatidylcholine (LPC) regioisomers, containing only a single FA at either the *sn*-1 or *sn*-2 position. Mass selected $[M+Na]^+$ adducts of LPC 18:1*n*-9(*cis*) isomers, differing only in the site of connection to the glycerol backbone, were separated using up to 40 passes around the cIMS device and subsequently subjected to CID (CE = 25 eV) in the transfer region. Figure 2(a) shows the separation of a mixture of LPC 18:1*n*-9(*cis*) isomers after 40 passes around the cIMS device, with two resolved features in the arrival time distribution. Integration of the two arrival-time features revealed differences in the underlying product ion mass spectra that enabled identification of the *sn*-position of the FA18:1 acyl chain on the glycerol backbone. The CID spectrum from the early feature (Figure 2b) showed a product ion at *m/z* 104, diagnostic for LPC 18:1/0:0, while the mass spectrum obtained by integrating the late feature (Figure 2c) showed a *m/z* 147 product ion, diagnostic for LPC 0:0/18:1.[31, 32] Interestingly, the observed ordering of the LPC isomers ion mobility separation is orthogonal to the separation observed in LC-MS based studies of LPC isomers, where LPC 0:0/18:1 elutes before LPC 18:1/0:0 on both reversed-phase [33] and hydrophobic interaction columns.[34]

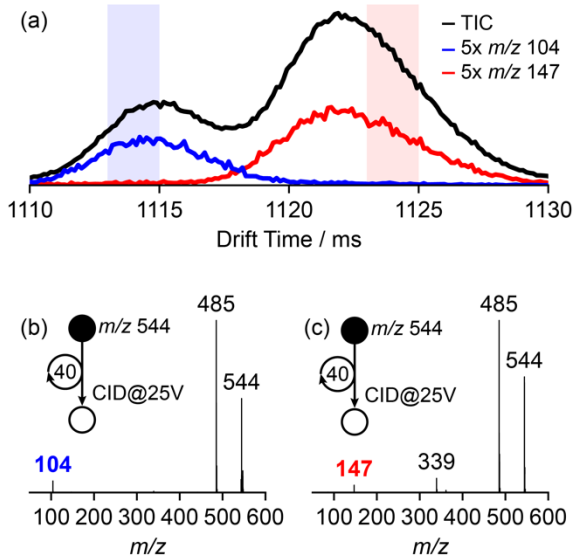

Figure 2. (a) Arrival time distribution of a mixture of LPC 18:1n-9(cis) isomers after 40 passes around the cIMS device. The total ion chromatogram is shown in black. (b) MS/MS spectrum between 1113 and 1115 ms and (c) 1123 and 1125 ms. Mass spectra were acquired using a collision energy of 25 eV in the transfer region of the instrument, post ion mobility.

To explore the utility of cyclic ion mobility to diacyl glycerophospholipids, methanolic stock solutions of six individual PC 34:1 isomers (i.e., three carbon-carbon double bond positions across two different *sn*-regioisomers) were

https://doi.org/10.26434/chemrxiv-2023-20nmh **ORCID:** https://orcid.org/0000-0002-0420-6116

infused separately *via* ESI. The [PC 34:1 + Na]$^+$ adducts (*m/z* 782.6) were mass selected, separated over 30-passes (~30 m total travelling distance) and subsequently collisionally activated (CE = 42.5 eV) in the transfer region prior to mass analysis. The arrival time distributions of the PC 16:0/18:1 isomers are shown in Figure 3(a). Similar to the arrival time order of the derivatized fatty acids, the PC 16:0/18:1*n*-7(*cis*) isomer has the earliest arrival time after 30 passes and is better resolved than the PC 16:0/18:1*n*-9(*cis*) and PC 16:0/18:1*n*-10(*cis*) pair. This trend is continued for the alternate set of *sn*-isomers, with PC 18:1*n*-7(*cis*)/16:0 having a shorter arrival time than PC 18:1*n*-9(*cis*)/16:0 and PC 18:1*n*-10(*cis*)/16:0. These observations parallel the behavior of these PC 34:1 isomers in reversed-phase liquid chromatography, where the *n*-7 isomers elute before *n*-9 or *n*-10, however all three double bond isomers are usually incompletely resolved (Figure S2). In each case studied here, the PC 16:0/18:1 isomer had a slightly shorter drift time than the corresponding PC 18:1/16:0 with the same double bond position. Such PC regioisomers are difficult to separate by reversed-phase HPLC, especially where the two fatty acyl chains are similar in carbon number and degree of unsaturation. Interesting, using 30 passes of the cIMS achieves a greater peak-to-peak resolution between *sn*-positional isomers than has previously been achieved by trapped-ion mobility spectrometry[17] providing an opportunity for isomer discovery in biological mixtures.

Infusion of a complex lipid extract from a LNCaP prostate cancer cell line displayed a single feature in the arrival time distribution of [PC 34:1+Na]$^+$ (Figure 4, black trace). The observed feature is broader than any of the individual PC 34:1 isomer standards acquired under the same conditions (Figure 4, colored traces), suggesting that the extract is comprised of a mixture of isomers.

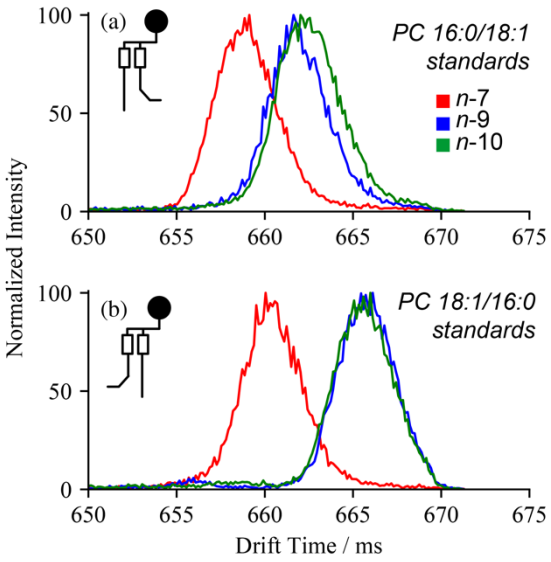

Figure 3. Arrival time distributions for [PC 34:1 +Na]$^+$ isomers (a) PC 16:0/18:1 and (b) PC 18:1/16:0 after 30 passes around the cIMS device.

The CID mass spectra presented in Figure S3 reveal that the ketene product ion at *m/z* 441 (arising from loss of FA 18:1) was more abundant for the PC 18:1/16:0 isomers, whereas the *m/z* 467 ketene product (arising from loss of FA 16:0) is more abundant for the PC 16:0/18:1 isomers.[35] For the PC34:1 standards, the relative proportion of *m/z* 441 (*i.e.*, $I_{441}/(I_{441}+I_{467})$) was observed to be 24±8 % for the PC 16:0/18:1 isomers, and 76±5 % for PC 18:1/16:0 (Figure S4 and S5). Previous studies have shown that the ratio of product ion abundances can be used to infer glycerophospholipid regioisomers in reversed-phase LCMS experiments.[36] This strategy was then used to determine the regioisomeric contributions to the PC 34:1 arrival time distribution in the LNCaP extract. Plotting the relative proportion of the *m/z* 441 product ion as a function of the arrival time indicated that most of the ion signal from the LNCaP lipid extract arises from PC 16:0/18:1, however at later drift time, where there remains a significant amount of ion signal intensity, the product ion ratio increases towards the ratio expected for the PC 18:1/16:0 isomers. This observation suggests that while the main ATD feature is comprised mostly of PC 16:0/18:1 isomers, there is an appreciable quantity of the non-canonical PC 18:1/16:0.

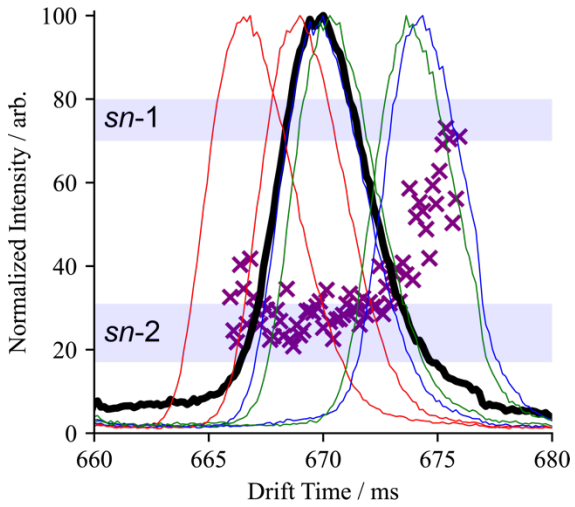

Figure 4. Arrival time distribution of [PC 34:1+Na]$^+$ from LNCaP cell extract (black trace) after 30 passes around the cIMS device. Crosses indicate the fractional abundance of m/z 441 diagnostic for 18:1 in the sn-1 position.

CONCLUSION

In this work, cyclic ion mobility has been used to effectively separate several types of lipid isomers. Multiple cIMS passes effectively separated fatty acids of identical acyl chain length, differing only in position or geometry of the carbon-carbon double bond. For both lyso- and diacylphosphatidylcholine, arrival time differences were found for isomers differing in both *sn*-position of acyl chains and the position of carbon-carbon double bonds.

Referencing the arrival time distribution of the [M+Na]$^+$ adduct of PC 34:1 from prostate cancer cell extracts to those obtained from high-purity lipid isomer reference standards, evidence for up to 6 different isomers was found. The ratio of diagnostic CID product ions indicated that while the majority of the observed PC 34:1 signal was from PC 16:0/18:1 isomers, a non-negligible proportion was from isomers of PC 18:1/16:0.

The ultra-high mobility resolution afforded by multiple cIMS passes effectively separate the different lipid isomer classes studied here. Increasingly, the structural diversity being uncovered in biological contexts includes lipids that have no commercially available reference standard, hampering unequivocal structural assignment based solely on retention time or drift time. Post-mobility collisional activation provided structurally diagnostic product ions for identification of *sn*-positional isomers. Coupling cIMS with alternative ion activation strategies, including UV-photdissociation[37] or ozone-induced dissociation,[38] offers an attractive possibility for separation and structural elucidation in a discovery-based workflow,[39] presenting a way to complete the picture of the lipidome.

ASSOCIATED CONTENT

Supporting Information

The Supporting Information is available free of charge on the ACS Publications website.

Tables containing travelling wave parameters and resolution calculations, mobility traces of negative mode fatty acyls, additional mass spectra and LC separation of PC 34:1 isomers (PDF)

AUTHOR INFORMATION

Corresponding Author

* berwyck.poad@qut.edu.au, (BLJP),
stephen.blanksby@qut.edu.au (SJB).

Present Addresses

†Present address School of Chemistry and Molecular Bioscience, University of Wollongong, NSW 2500, Australia.

Author Contributions

The manuscript was written through contributions of all authors.

ACKNOWLEDGMENT

This work was supported by funding from the Australian Research Council (Grant numbers LP180100238, LE220100031). Some of the data presented here was acquired in the Central Analytical Research Facility (CARF) at Queensland University of Technology (QUT), operated by the QUT Division of Research Infrastructure.

REFERENCES

(1) Wenk, M. R. Lipidomics: new tools and applications. *Cell* **2010**, *143* (6), 888-895.
(2) Shevchenko, A.; Simons, K. Lipidomics: coming to grips with lipid diversity. *Nature Rev Mol Cell Biol* **2010**, *11* (8), 593-598.
(3) Blanksby, S. J.; Mitchell, T. W. Advances in mass spectrometry for lipidomics. *Ann Rev Anal Chem* **2010**, *3*, 433-465.
(4) Heiles, S. Advanced tandem mass spectrometry in metabolomics and lipidomics. *Anal Bioanal Chem* **2021**, *413* (24), 5927-5948.
(5) Hancock, S. E.; Poad, B. L. J.; Batarseh, A.; Abbott, S. K.; Mitchell, T. W. Advances and unresolved challenges in the structural characterization of isomeric lipids. *Analytical Biochemistry* **2017**, *524*, 45-55. DOI: 10.1016/j.ab.2016.09.014.
(6) Huynh, K.; Barlow, C. K.; Jayawardana, K. S.; Weir, J. M.; Mellett, N. A.; Cinel, M.; Magliano, D. J.; Shaw, J. E.; Drew, B. G.; Meikle, P. J. High-Throughput Plasma Lipidomics: Detailed Mapping of the Associations with Cardiometabolic Risk Factors. *Cell Chemical Biology* **2019**, *26* (1), 71-84.e74. DOI: 10.1016/j.chembiol.2018.10.008.
(7) Bowman, A. P.; Abzalimov, R. R.; Shvartsburg, A. A. Broad Separation of Isomeric Lipids by High-Resolution Differential Ion Mobility Spectrometry with Tandem Mass Spectrometry. *Journal of the American Society for Mass Spectrometry* **2017**, *28* (8), 1552-1561. DOI: 10.1007/s13361-017-1675-2.
(8) Paglia, G.; Kliman, M.; Claude, E.; Geromanos, S.; Astarita, G. Applications of ion-mobility mass spectrometry for lipid analysis. *Analytical and Bioanalytical Chemistry* **2015**, *407* (17), 4995-5007. DOI: 10.1007/s00216-015-8664-8.
(9) Kim, H. I.; Kim, H.; Pang, E. S.; Ryu, E. K.; Beegle, L. W.; Loo, J. A.; Goddard, W. A.; Kanik, I. Structural Characterization of Unsaturated Phosphatidylcholines Using Traveling Wave Ion Mobility Spectrometry. *Analytical Chemistry* **2009**, *81* (20), 8289-8297. DOI: 10.1021/ac900672a.
(10) Groessl, M.; Graf, S.; Knochenmuss, R. High resolution ion mobility-mass spectrometry for separation and identification of isomeric lipids. *Analyst* **2015**, *140* (20), 6904-6911, 10.1039/C5AN00838G. DOI: 10.1039/C5AN00838G.
(11) Rivera, E. S.; Djambazova, K. V.; Neumann, E. K.; Caprioli, R. M.; Spraggins, J. M. Integrating ion mobility and imaging mass spectrometry for comprehensive analysis of biological tissues: A brief review and perspective. *Journal of Mass Spectrometry* **2020**, *55* (12), e4614. DOI: 10.1002/jms.4614.
(12) Ujma, J.; Ropartz, D.; Giles, K.; Richardson, K.; Langridge, D.; Wildgoose, J.; Green, M.; Pringle, S. Cyclic Ion Mobility Mass Spectrometry Distinguishes Anomers and Open-Ring Forms of Pentasaccharides. *Journal of The American Society for Mass Spectrometry* **2019**, *30* (6), 1028-1037. DOI: 10.1007/s13361-019-02168-9.
(13) Rüger, C. P.; Le Maître, J.; Maillard, J.; Riches, E.; Palmer, M.; Afonso, C.; Giusti, P. Exploring Complex Mixtures by Cyclic Ion Mobility High-Resolution Mass Spectrometry: Application Toward Petroleum. *Analytical Chemistry* **2021**, *93* (14), 5872-5881. DOI: 10.1021/acs.analchem.1c00222.
(14) Christofi, E.; Barran, P. Ion Mobility Mass Spectrometry (IM-MS) for Structural Biology: Insights Gained by Measuring Mass, Charge, and Collision Cross Section. *Chemical Reviews* **2023**. DOI: 10.1021/acs.chemrev.2c00600.
(15) Jeanne Dit Fouque, K.; Fernandez-Lima, F. Recent advances in biological separations using trapped ion mobility spectrometry – mass spectrometry. *TrAC Trends in Analytical Chemistry* **2019**, *116*, 308-315. DOI: 10.1016/j.trac.2019.04.010.

(16) Dubland, J. A. Lipid analysis by ion mobility spectrometry combined with mass spectrometry: A brief update with a perspective on applications in the clinical laboratory. *Journal of Mass Spectrometry and Advances in the Clinical Lab* **2022**, *23*, 7-13. DOI: 10.1016/j.jmsacl.2021.12.005.
(17) Jeanne Dit Fouque, K.; Ramirez, C. E.; Lewis, R. L.; Koelmel, J. P.; Garrett, T. J.; Yost, R. A.; Fernandez-Lima, F. Effective Liquid Chromatography–Trapped Ion Mobility Spectrometry–Mass Spectrometry Separation of Isomeric Lipid Species. *Analytical Chemistry* **2019**, *91* (8), 5021-5027. DOI: 10.1021/acs.analchem.8b04979.
(18) Bollinger, J. G.; Rohan, G.; Sadilek, M.; Gelb, M. H. LC/ESI-MS/MS detection of FAs by charge reversal derivatization with more than four orders of magnitude improvement in sensitivity. *Journal of Lipid Research* **2013**, *54* (12), 3523-3530. DOI: 10.1194/jlr.D040782.
(19) Young, R. S. E.; Flakelar, C. L.; Narreddula, V. R.; Jekimovs, L. J.; Menzel, J. P.; Poad, B. L. J.; Blanksby, S. J. Identification of Carbon-Carbon Double Bond Stereochemistry in Unsaturated Fatty Acids by Charge-Remote Fragmentation of Fixed-Charge Derivatives. *Analytical Chemistry* **2022**, *94* (46), 16180-16188. DOI: 10.1021/acs.analchem.2c03625.
(20) Velosa, D. C.; Dunham, A. J.; Rivera, M. E.; Neal, S. P.; Chouinard, C. D. Improved Ion Mobility Separation and Structural Characterization of Steroids using Derivatization Methods. *Journal of the American Society for Mass Spectrometry* **2022**. DOI: 10.1021/jasms.2c00164.
(21) Hynds, H. M.; Hines, K. M. Ion Mobility Shift Reagents for Lipid Double Bonds Based on Paternò–Büchi Photoderivatization with Halogenated Acetophenones. *Journal of the American Society for Mass Spectrometry* **2022**, *33* (10), 1982-1989. DOI: 10.1021/jasms.2c00211.
(22) Liebisch, G.; Fahy, E.; Aoki, J.; Dennis, E. A.; Durand, T.; Ejsing, C. S.; Fedorova, M.; Feussner, I.; Griffiths, W. J.; Köfeler, H.; et al. Update on LIPID MAPS classification, nomenclature, and shorthand notation for MS-derived lipid structures. *Journal of Lipid Research* **2020**, *61* (12), 1539-1555. DOI: 10.1194/jlr.S120001025.
(23) The nomenclature of lipids (recommendations 1976). *Journal of Lipid Research* **1978**, *19* (1), 114-128. DOI: 10.1016/S0022-2275(20)41583-4.
(24) Dubois, N.; Barthomeuf, C.; Bergé, J.-P. Convenient preparation of picolinyl derivatives from fatty acid esters. *European Journal of Lipid Science and Technology* **2006**, *108* (1), 28-32. DOI: 10.1002/ejlt.200501217.
(25) Destaillats, F.; Angers, P. One-step methodology for the synthesis of FA picolinyl esters from intact lipids. *Journal of the American Oil Chemists' Society* **2002**, *79* (3), 253-256. DOI: 10.1007/s11746-002-0469-7.
(26) Young, R. S. E.; Bowman, A. P.; Williams, E. D.; Tousignant, K. D.; Bidgood, C. L.; Narreddula, V. R.; Gupta, R.; Marshall, D. L.; Poad, B. L. J.; Nelson, C. C.; et al. Apocryphal FADS2 activity promotes fatty acid diversification in cancer. *Cell Reports* **2021**, *34* (6), 108738. DOI: 10.1016/j.celrep.2021.108738.
(27) Giles, K.; Ujma, J.; Wildgoose, J.; Pringle, S.; Richardson, K.; Langridge, D.; Green, M. A Cyclic Ion Mobility-Mass Spectrometry System. *Analytical Chemistry* **2019**, *91* (13), 8564-8573. DOI: 10.1021/acs.analchem.9b01838.
(28) Dodds, J. N.; May, J. C.; McLean, J. A. Correlating Resolving Power, Resolution, and Collision Cross Section: Unifying Cross-Platform Assessment of Separation Efficiency in Ion Mobility Spectrometry. *Analytical Chemistry* **2017**, *89* (22), 12176-12184. DOI: 10.1021/acs.analchem.7b02827.
(29) Harvey, D. J. Picolinyl esters as derivatives for the structural determination of long chain branched and unsaturated fatty acids. *Biomedical Mass Spectrometry* **1982**, *9* (1), 33-38. DOI: 10.1002/bms.1200090107.
(30) Kirschbaum, C.; Young, R. S. E.; Greis, K.; Menzel, J. P.; Gewinner, S.; Schöllkopf, W.; Meijer, G.; von Helden, G.; Causon, T.; Narreddula, V. R.; et al. Establishing carbon–carbon double bond position and configuration in unsaturated fatty acids by gas-phase infrared spectroscopy. *Chemical Science* **2023**, *14*, 2518-2527. DOI: 10.1039/D2SC06487A.
(31) Han, X.; Gross, R. W. Structural Determination of Lysophospholipid Regioisomers by Electrospray Ionization Tandem Mass Spectrometry. *Journal of the American Chemical Society* **1996**, *118* (2), 451-457. DOI: 10.1021/ja952326r.
(32) Hsu, F.-F.; Turk, J.; Thukkani, A. K.; Messner, M. C.; Wildsmith, K. R.; Ford, D. A. Characterization of alkylacyl, alk-1-enylacyl and lyso subclasses of glycerophosphocholine by tandem quadrupole mass spectrometry with electrospray ionization. *Journal of Mass Spectrometry* **2003**, *38* (7), 752-763. DOI: 10.1002/jms.491.
(33) Creer, M. H.; Gross, R. W. Separation of isomeric lysophospholipids by reverse phase HPLC. *Lipids* **1985**, *20* (12), 922-928. DOI: 10.1007/BF02534778.
(34) Koistinen, K. M.; Suoniemi, M.; Simolin, H.; Ekroos, K. Quantitative lysophospholipidomics in human plasma and skin by LC–MS/MS. *Analytical and Bioanalytical Chemistry* **2015**, *407* (17), 5091-5099. DOI: 10.1007/s00216-014-8453-9.
(35) Murphy, R. C. Ch 5: Glycerophospholipids. In *Tandem Mass Spectrometry of Lipids: Molecular Analysis of Complex Lipids*, The Royal Society of Chemistry, 2015; pp 130-193.
(36) Wozny, K.; Lehmann, W. D.; Wozny, M.; Akbulut, B. S.; Brügger, B. A method for the quantitative determination of glycerophospholipid regioisomers by UPLC-ESI-MS/MS. *Analytical and Bioanalytical Chemistry* **2019**, *411* (4), 915-924. DOI: 10.1007/s00216-018-1517-5.
(37) Williams, P. E.; Klein, D. R.; Greer, S. M.; Brodbelt, J. S. Pinpointing Double Bond and sn-Positions in Glycerophospholipids via Hybrid 193 nm Ultraviolet Photodissociation (UVPD) Mass Spectrometry. *Journal of the American Chemical Society* **2017**, *139* (44), 15681-15690. DOI: 10.1021/jacs.7b06416.
(38) Poad, B. L. J.; Green, M. R.; Kirk, J. M.; Tomczyk, N.; Mitchell, T. W.; Blanksby, S. J. High-Pressure Ozone-Induced Dissociation for Lipid Structure Elucidation on Fast Chromatographic Timescales. *Analytical Chemistry* **2017**, *89* (7), 4223-4229. DOI: 10.1021/acs.analchem.7b00268.

(39) Menzel, J. P.; Young, R. S. E.; Benfield, A. H.; Scott, J.; Butler, L. M.; Henriques, S. T.; Poad, B. L. J.; Blanksby, S. J. OzFAD: Ozone-enabled fatty acid discovery reveals unexpected diversity in the human lipidome. *bioRxiv* **2022**, 2022.2010.2024.513604. DOI: 10.1101/2022.10.24.513604.